American Journal of Chemical Engineering
2022; 10(1): 1-10
http://www.sciencepublishinggroup.com/j/ajche
doi: 10.11648/j.ajche.20221001.11
ISSN: 2330-8605 (Print); ISSN: 2330-8613 (Online)

The Partial Oxidation of Methane to Hydrogen over M(1)-Ni(5)/AlCeO$_3$(M=Ce, La, Y) Catalysts

Ho Joon Seo

Department of Chemical and Biomolecular Engineering, Chonnam National University, Yosu, Republic of Korea

Email address:
hjseo@jnu.ac.kr

To cite this article:
Ho Joon Seo. The Partial Oxidation of Methane to Hydrogen over M(1)-Ni(5)/AlCeO$_3$(M=Ce, La, Y) Catalysts. *American Journal of Chemical Engineering.* Vol. 10, No. 1, 2022, pp. 1-10. doi: 10.11648/j.ajche.20221001.11

Received: December 3, 2021; **Accepted**: February 23, 2022; **Published**: March 4, 2022

Abstract: The catalytic yields of partial oxidation of methane (POM) to hydrogen over M(1)-Ni(5)/Al$_2$O$_3$(M=, Ce, La, Y) catalysts were investigated using a fixed bed flow reactor under atmospheric pressure to solve the global warming problem and clean energy demand. Catalyst activity is evaluated by performing the reaction of POM to hydrogen, and active sites of the catalyst are verified by instrumental analysis. The catalysts were characterized by XPS, XRD, FESEM, EDS, FETEM. The crystal phase behavior of reduced La(1)-Ni(5)/AlCeO$_3$ catalysts before and after the reaction were studied by XRD analysis. The crystalline phase of Ni and La on La(1)-Ni(5)/AlCeO$_3$ reduced before reaction was not obserbed due to uniform distribution of nanoparticles. FESEM and EDS analyses show that nanoparticles of Ni, La and Ce are uniformly distributed on the catalyst surface. In addition, TEM images and EDS mapping of La, Ni, Ce, O, and Al for a reduced La(1)-Ni(5)/AlCeO$_3$ catalyst before reaction show that the elements are well distributed. When 1 wt% of La was added to Ni(5)/AlCeO$_3$ catalyst, XPS results showed that O^-, $O_{vacancy}$, and O_2^- species, Ni$_2$p$_{3/2}$, and Ce3d$_{5/2}$ increased 1.4, 52.7, 6.3% on the La(1)- Ni(5)/ AlCeO$_3$ catalyst, respectively. The yield of hydrogen on the La(1)- Ni(5)/ AlCeO$_3$ catalyst was 89.1%, which was much better than that of M(1)-Ni(5)/Al$_2$O$_3$(M=Ce, Y) catalysts. As Ce^{4+}/Ce^{3+} ions in CeO$_2$ produced by the reaction of AlCeO$_3$ with oxygen were substitute to La^{3+}, Ni^{2+}, it made oxygen vacancies in the lattice and further improved the hydrogen yield by increasing the dispersion of Ni atoms with strong metal- support interaction (SMSI) effect.

Keywords: Hydrogen, Lanthanum, Partial Oxidation of Methane, Nickel, AlCeO$_3$

1. Introduction

The partial oxidation reaction of methane is of great interest because of the increasing global demand for hydrogen energy and environmental problems caused by global warming. [1-5] Methane, a major component of natural gas, is an important hydrocarbon feedstock for fuel and chemical synthesis. However, since the C-H bond energy of methane is 413 kJmol^{-1}, a lot of energy is required to activate methane and synthesize hydrogen energy and necessary chemicals through a chemical reaction. Most of today's hydrogen is obtained from methane-steam reforming reaction [6-10], Equation (1) under the reaction conditions of 700°C-1000°C and 3-25 atm over a catalyst. In addition, since this reaction is endothermic, a large amount of energy is consumed. On the other hand, the partial oxidation of methane [11-15], Equation (2) reacts with methane using less than stoichiometric amount of oxygen to obtain hydrogen. This reaction is exothermic and occurs more rapidly than methane-steam reforming and the reactor size is small. Both the steam reforming reaction and the partial oxidation reaction is accompanied by a water gas shift reaction [16-20], Equation (3) during the reaction.

$$CH_4 + H_2O \rightarrow CO + 3H_2,\ \widehat{\Delta H^0_{298}}=207\ \text{k J/mol} \quad (1)$$

$$2CH_4 + O_2 \rightarrow 2CO + 4H_2,\ \widehat{\Delta H^0_{298}}=-36\ \text{k J/mol} \quad (2)$$

$$CO + H_2O \rightarrow CO_2 + H_2,\ \widehat{\Delta H^0_{298}}=-41\ \text{k J/mol} \quad (3)$$

Noble metal catalysts such as Rh, Pd, Ru, Ir are highly active catalysts for producing hydrogen [21-25] and syngas [26-30] by activating methane in the POM reaction, but they cost a lot and small amount. Therefore, There is a need to develop a catalyst of POM for hydrogen production. Transition metals such as Fe, Co, and Ni have good catalyst of activity in the hydrogenation reaction of methane and are

much cheaper than precious metal catalysts, so they are widely used to study the activation of methane. In particular, the Ni catalyst is known as a catalyst for increasing the hydrogen yield in the production of hydrogen from methane. However, the nickel catalyst has good initial activity, but methane decomposition, Equation 4 and CO disproportionation reaction, Equation 5, drastically reduces the activity of the catalyst with a lot of carbon deposition.

$$CH_4 \rightarrow C + 2H_2,\ \widehat{\Delta H_{298}^0}=75.6\ k\ J/mol \quad (4)$$

$$2CO \rightarrow C + CO_2,\ \widehat{\Delta H_{298}^0}=-172.4\ k\ J/mol \quad (5)$$

In addition, The rapid deactivation of the catalyst is occurring due to the sintering of nickel particles by the low Tammann temperature. [31] Therefore, in order to improve the activity and stability of the Ni catalyst for POM, it is very important to select the catalyst carrier and co-catalyst. Tsubaki et al. [32] has been reported that co-catalyst of oxides of alkali and alkaline earth metals and rare earth metals on nickel catalysts prevent carbon deposition and improve catalyst stability. In addition, research results suggest that rare earth metals contribute to the improvement of oxygen storage capacity, oxygen vacancy formation, thermal stability of alumina carriers, and dispersion of active species. [33, 34] It is known that lanthanide oxides, which are rare earth metals, have an f orbital electron configuration and affect the basic strength of catalysts. [35] Gong et al. [36] reported that a Ni-based regular mesoporous catalyst modified with La has SMSI effect, prevents carbon deposition on the catalyst and improves the basicity of the catalyst. There is also a study result that the lanthanum promoter reduces the chemical bond between the carrier and Ni due to the SMSI effect. [37-42] This lanthanum metal is thought to have chemical properties that can serve as a co-catalyst of the Ni catalyst of POM. To develop a catalyst that maintains catalytic activity and thermal stability to improve hydrogen yield for a long period of time and prevents carbon deposition, Ni is used as an active material of the catalyst and La, Ce, Y are used as a co-catalyst. $AlCeO_3$ containing Ce, which has strong metal-support reducing ability and ability to supply oxygen species to the surface of the catalyst, is used as the carrier of the catalyst. We intend to evaluate the activity of the catalyst for hydrogen production by preparing the catalyst by the impregnation method using the citric acid method and performing the POM reaction using a fixed-bed flow-through reactor under atmospheric pressure. We want to verify the result by analyzing the catalyst's active sites by means of instrumentation such as XRD, XPS, and FESEM, EDS, FETEM.

2. Experimental

2.1. Catalyst Preparation

The M(1)-Ni(5)/$AlCeO_3$ (M=La, Ce, Y) catalyst was prepared using a standard impregnation method. Then, it was prepared as follows. The numbers in parentheses indicate the weight percent loaded. After dissolving $Ni(NO_3)_2{\cdot}6H_2O$ (0.025 g), $La(NO_3)_3{\cdot}6H_2O$ (0.003 g), $Ce(NO_3){\cdot}6H_2O$ (0.003 g), $Y(NO_3)_2{\cdot}6H_2O$ (0.004 g), the complexing agent, citric acid/(M + Ni)=1.5 M in ethanol added, and 0.1 g of the $AlCeO_3$ carrier was added to the reactor. The mixture was uniformly mixed with a stirrer for 5h. Precipitation obtained after filtration was dried in a dryer at 100°C for 24 h. The dried sample was calcined in an electric furnace (TMF-1000, Eyela Co., Japan) at 773 K for 5 h. After making a M(1)-Ni(5)/$AlCeO_3$ (M=La, Ce, Y) catalyst, it was crushed to 150 ~200 mesh and used.

2.2. Catalyst Characterization

XRD patterns were obtained using a Panalytical Empyrean 3D high-resolution X-ray diffractometer (Cu Ka radiation, λ=1.5419 Å, 40 kV, 30 mA). XPS spectra were obtained as Alkα X-rays using an HP-X-ray photoelectron spectrometer (Thermo Scientific K-Al-pha+) under operating conditions of 1×10^{-9} mbar and 1.75 keV. FESEM images were obtained using a field emission scanning microscope of a Zeiss Sigma 500 model, and the chemical composition of the catalyst was analyzed with an EDS detector. FETEM images were obtained using a Jeol Jem-2100F at an accelerating voltage of 200 kV, and were obtained layered images and K or L series images of each elements of catalyst by analyzing using EDS (X-MaxNT, 80T model, UK).

2.3. Catalyic Activity Test

The catalytic reaction is carried out at atmospheric pressure using a fixed-bed flow reactor. The powder catalyst, 0.05 g is put on the quartz wool in a quartz reactor with an inner diameter of 10 mm. The process variables such as reaction temperature, pressure, CH_4/O_2 molar ratio, and GHSV were 973 K, 1 atm, 2, 1.08×10^5 ml/gcat.·h, respectively. The desired temperature of the reactor is placed a K-type thermocouple on the catalyst in the reactor and controlled within the range of ± 1 K using a PID controller. The composition of the reactants is controlled using a mass flow meter after purging the reactants using a pressure gauge attached to each cylinder. The product was analyzed by TCD by connecting a column of Porapak Q and Molecular sieve 5A in parallel to a GC (Shimadzu Co., Model 14B, Japan). After the catalyst was reduced at 773 K for 5h by hydrogen sended at a flow rate of 20 mlH_2/min, it was used by increasing the reaction temperature at a rate of 283 K/min

3. Results and Discussion

3.1. Catalyst Characterization

The atomic % of core electron levels for Ni(5)/$AlCeO_3$ and La(1)-Ni(5)/$AlCeO_3$ catalyst before reaction are summarized in Table 1. The 1 wt% addition of La to the Ni(5)/$AlCeO_3$ catalyst was found that the atoms of $Ni_2p_{3/2}$ increased from 0.93% to 1.42%, and the atoms of $Ce3d_{5/2}$ increased from 1.28% to 1.36%. It is believed to increase the dispersion of Ni and Ce atoms due to creating oxygen vacancies by some of Ce^{4+} ions in CeO_2 substituted by La^{3+} in the lattice. Alvarez-Galvan et al. [43] has been reported that the lattice modification of CeO_2 by La increased the dispersion of metals and the storage capacity of

oxygen on the carrier. Figure 1 shows the XRD patterns of the reduced La(1)-Ni(5)/$AlCeO_3$ catalyst before and after the reaction. The characteristic peaks of CeO_2 were shown in the reduced catalyst before the reaction at 2θ=28.6, 33.1, 47.5, 56.3, at 59.1, 69.4, and 76.7°, but them of CeO_2 after the reaction were shown at 2θ=28.7, 33.2, 47.6, 56.4, 59.1, 69.4, 76.7, 79.1, 88.3°. The crystalline phase of Ni and La on reduced La(1)-Ni(5)/$AlCeO_3$ before reaction was not observed. Characteristic peaks of Ni metal crystalline phase were appeared at 2θ=44.7, 51.0, 51.9° and them of the NiO crystal phase were appeared at 2θ=43.8, 62.8, and 74.6° after reaction. The nickel aluminate phase, $NiAl_2O_4$ was observed at 2θ=35.6° This phenomenon could be caused by the SMSI effect between NiO and $AlCeO_3$ by the addition of 1 wt% of La in Ni(5)/$AlCeO_3$ catalyst. In addition, $AlCeO_3$ can be oxidized to CeO_2 by heating under oxygen and CeO_2 can be reduced by heating under hydrogen. It is thought that the nanoparticles of Ni by Ce^{4+}/Ce^{3+} are well dispersed on the catalyst surface. It was found to be consistent with the results of FESEM and FETEM, EDS. Figure 2 shows the XPS Spectra of O1s, Al2p, Ce3d, Ni2p, La3d core electron levels of La(1)-Ni(5)/$AlCeO_3$ catalyst reduced before reaction. The characteristic peaks of O1s appeared at 529.4, 530.9, and 531.9 eV, and were O_2^-, $O_{vacancy}$, O^-, respectively. This change in oxygen species resulted in changing the lattice constant of catalyst carrier generated by the incorporation of La^{3+}(11.6 nm), Ni^{2+}(6.9 nm) with different ionic radii in the CeO_2(Ce^{4+}, 9.7 nm) lattice. Increasing of the oxygen mobility by changing the lattice constant of catalyst carrier could be considered to improve the stability of the catalyst. The characteristic peaks of Al 2p appeared at 73.68, 74.18, and 74.78 eV, and they were Al(metal), Al_2O_3, $Al(OH)_3$, respectively. The characteristic peaks of $Ce3d_{3/2}$ appeared at 900.5 and 915 eV were Ce^{3+} and Ce^{4+}, respectively. The characteristic peak of $Ce3d_{5/2}$ appeared at 897.96 eV was Ce^{4+}. In addition, the catalyst carrier, $AlCeO_3$, is occurred reversibly by the following chemical formula, Equation (6). [44]

Table 1. *Atomic % of Core Electron Levels for for Ni(5)/$AlCeO_3$ and La(1)-Ni(5)/$AlCeO_3$ catalyst before reaction.*

Name of core Electron levels	Atomic % of Ni(5)/$AlCeO_3$	Atomic % of La(1)-Ni(5)/$AlCeO_3$
$La3d_{5/2}$	-	0.03
$Ni_2p_{3/2}$	0.93	1.42
$Ce3d_{5/2}$	1.28	1.36
O1s	73.17	74.16
Al2p	24.62	23.02

$$4AlCeO_3 + O_2 \rightleftarrows 4CeO_2 + 2Al_2O_3 \quad (6)$$

The CeO_2 produced in this reaction promotes the dispersion of Ni on the catalyst by redox reaction of Ce^{3+}/Ce^{4+}, and had the ability to store and release an O_2. Damyanova et al. [45] have reported that Ni/xCeO_2-Al_2O_3 catalyst with ions of Ni^{2+}/Ni^0 and Ce^{3+}/Ce^{4+} has high activity, stability, and resistance to carbon deposition because it is dispersed 4.7~6.3 nm particles than Ni/Al_2O_3 on the catalyst surface. It was reported that Ce^{3+} made by reduction reaction of CeO_2 with Ce^{4+} ions creates defects of Al-O-Ce, which can act as the sites of the growth of NiO, and prevents sintering of particles due to SMSI effect. [46] Venezia et al. [47] reported that introducing Ni^{2+} (6.9 nm, ionic radius) into the lattice of CeO_2 with Ce^{4+} ions (9.7 nm, ionic radius) decresed lattice constant. These phenomena could be created oxygen vacancies and increased the mobility of oxygen to prevent carbon deposition on the surface. The characteristic peaks of $Ni2p_{3/2}$ were found at 851.3, 854.1, 855.8, and 861.3 eV, and they were Ni metal, NiO, $NiAl_2O_4$, and Ni satallite, respectively. Characteristic peaks of $Ni2p_{1/2}$ appeared at 874.1 eV. The characteristic peaks of $NiAl_2O_4$ could be considered as NiO interaction with carrier, $AlCeO_3$. M. A. Goula et al [46] were reported that metal-support interactions are important in defining the catalytic properties. Characteristic peaks of $La3d_{5/2}$ appeared at 833.7, 834.8 eV, and their species were La^{3+} and La^{3+} satellite. FESEM images and EDS characteristic peaks of La(1)-Ni(5)/$AlCeO_3$ catalysts reduced before reaction at 773 K were shown in Figures 3 and 4. It was found that spherical nanoparticles were uniformly distributed on the catalyst surface. It was confirmed that particles of Ce, Al, O, La, Ni were present on the catalyst surface. Figure 5 shows the representative TEM images for a reduced La(1)-Ni(5)/$AlCeO_3$ catalyst before reaction. As shown in Figure 5, the elements of La, Ni, Ce were well distributed on the catalyst surface. In order to explore in more detail the distribution of La, Ni, Ce, O, Al elements on the catalytic surface, the mapping images of catalyst have been observed. Figures 6 and 7 show EDS mapping of La, Ni, Ce, O, and Al on the catalyst surface, and it can be seen that the elements of nanoparticle are well distributed.

3.2. Catalyst Activity

Figure 8 is shown for the hydrogen yield for the reaction time of the M(1)-Ni(5)/$AlCeO_3$ (M=Ce, La, Y) catalyst. The activity of the catalyst was in the order of La(1)-Ni(5)/$AlCeO_3$ >>Ni(10)/$AlCeO_3$>>Y(1)-Ni(5)/$AlCeO_3$> Ce(1)-Ni(5)/$AlCeO_3$> Ni(5)/$AlCeO_3$. When 1 wt% of La was added on Ni(5)/$AlCeO_3$ catalyst, the highest hydrogen yield, 89.1% was obtained. It is believed that this phenomenon is enhanced the reduction of NiO particles by adding La to Ni-Al and Ni-Ce and uniformly dispersed Ni^0 on the catalyst surface by SMSI effect. [48] The H_2 yield was calculated based on Equation (7):

$$\%\ H2\ yield = \frac{H_2\ mol\ produced}{mol\ of\ methane\ in\ the\ feedstock} \times 100 \quad (7)$$

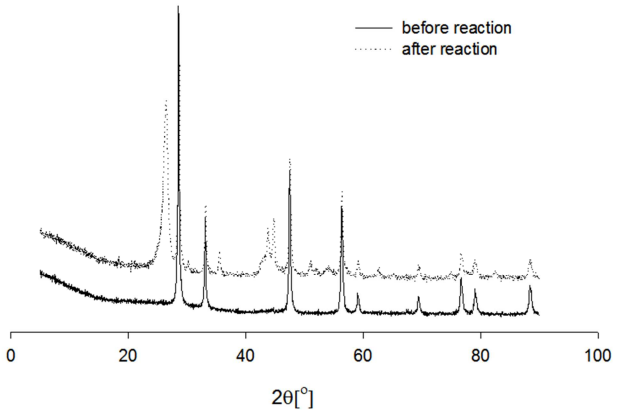

Figure 1. *XRD patterns of reduced La (1) – Ni (5)/$AlCeO_3$ catalyst before and after reaction.*

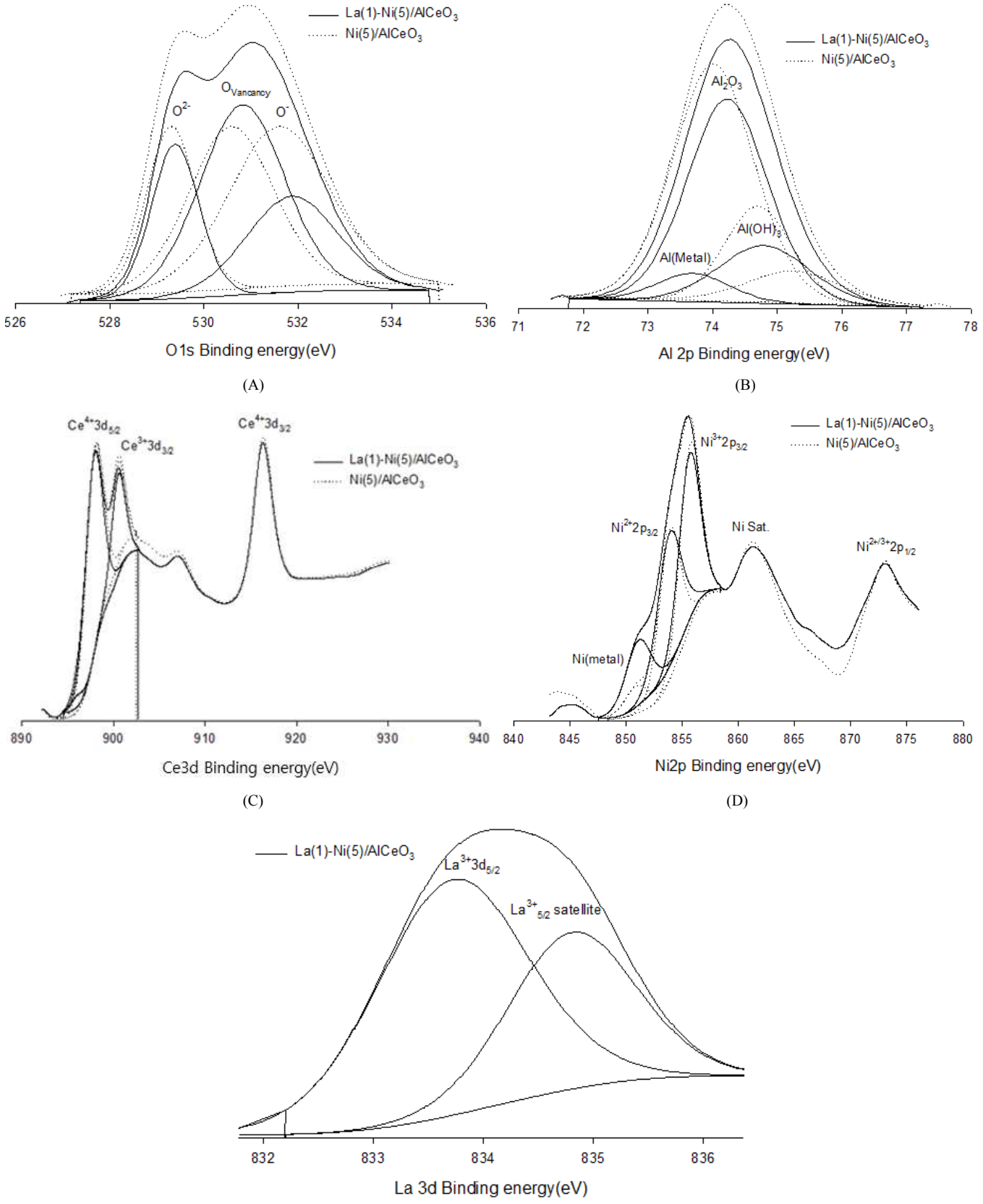

Figure 2. *XPS spectra of (A) O1s, (B) Al2p, (C) Ce3d, (D) Ni2p, (E) La3d core electron levels for reduced La(1)-Ni(5)/AlCeO$_3$ and Ni(5)/AlCeO$_3$ catalyst before reaction.*

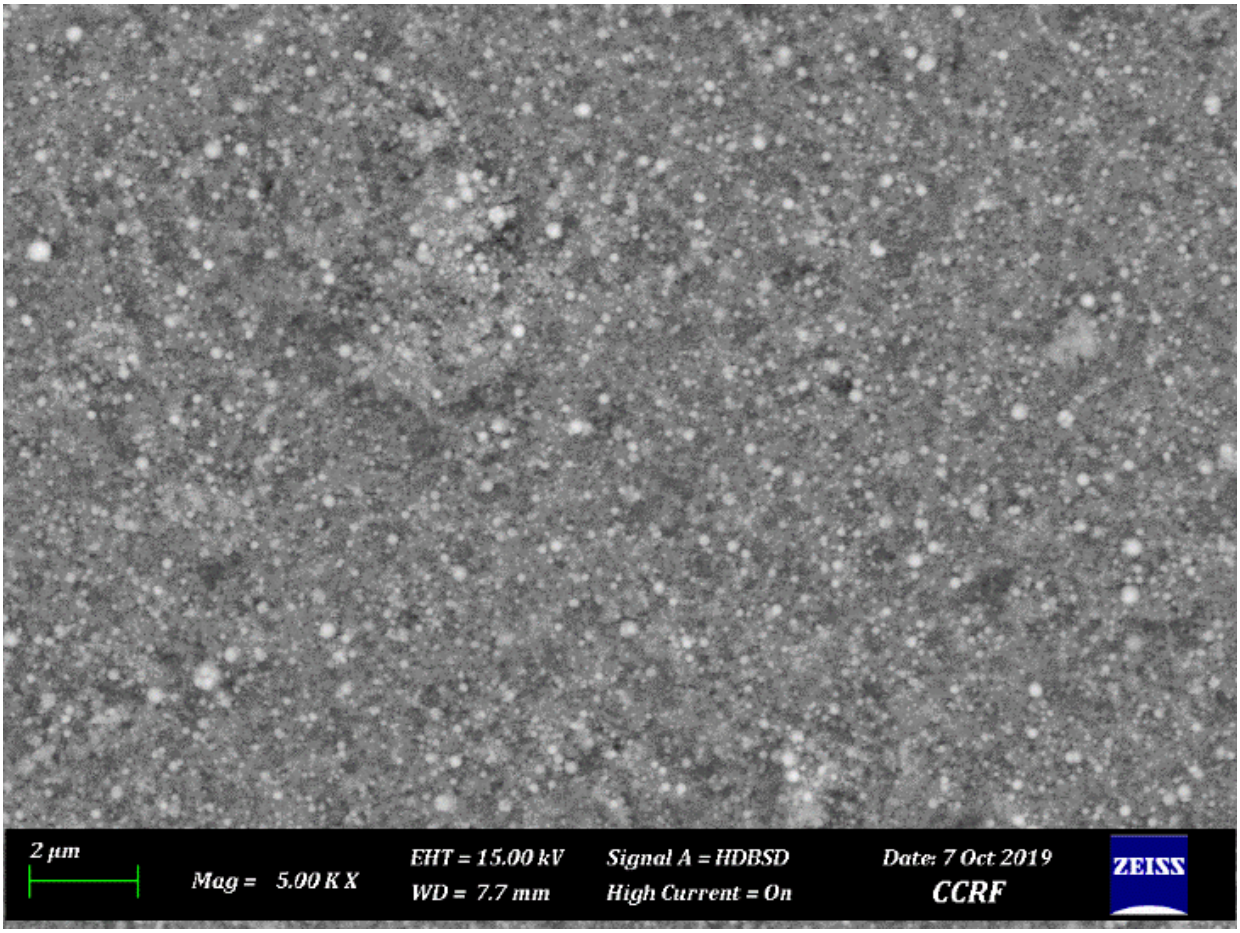

Figure 3. *FESEM image of reduced La(1)-Ni(5)/AlCeO₃ catalyst before reaction.*

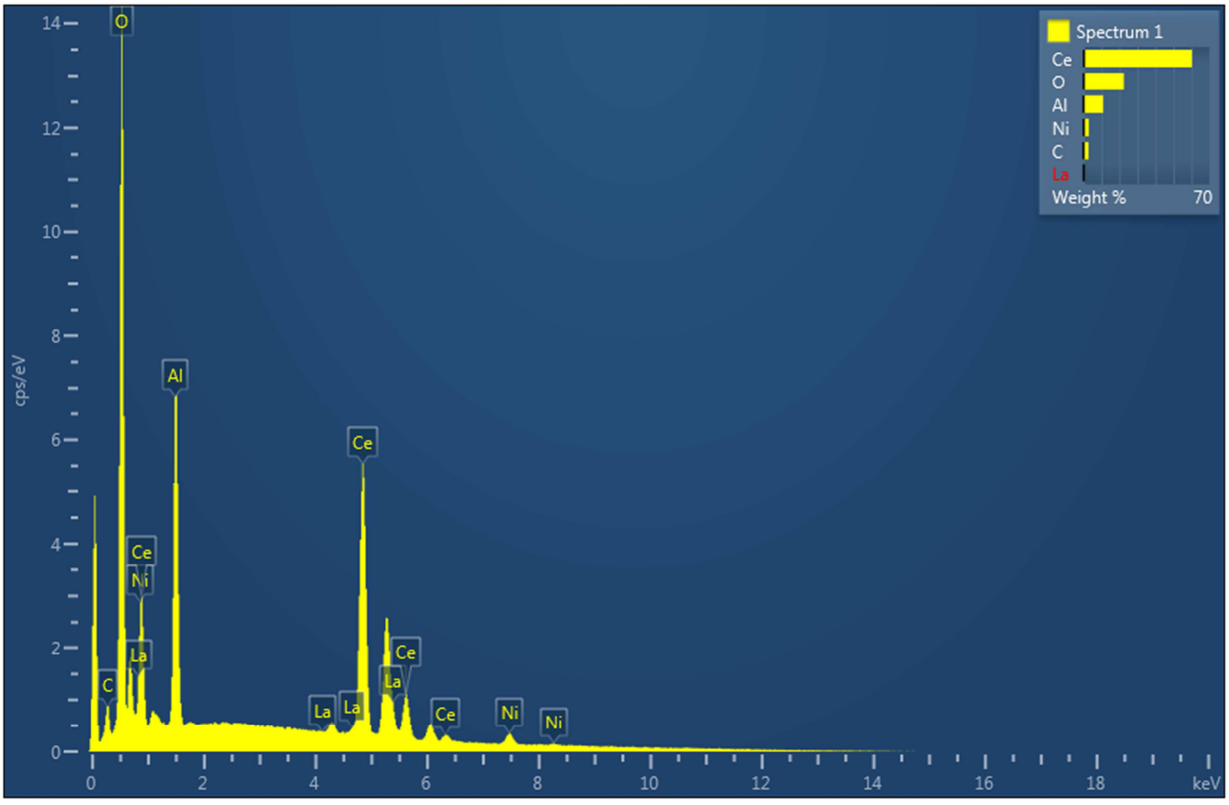

Figure 4. *EDS characteristic peaks on surface of reduced La(1)-Ni(5)/AlCeO₃ catalyst before reaction.*

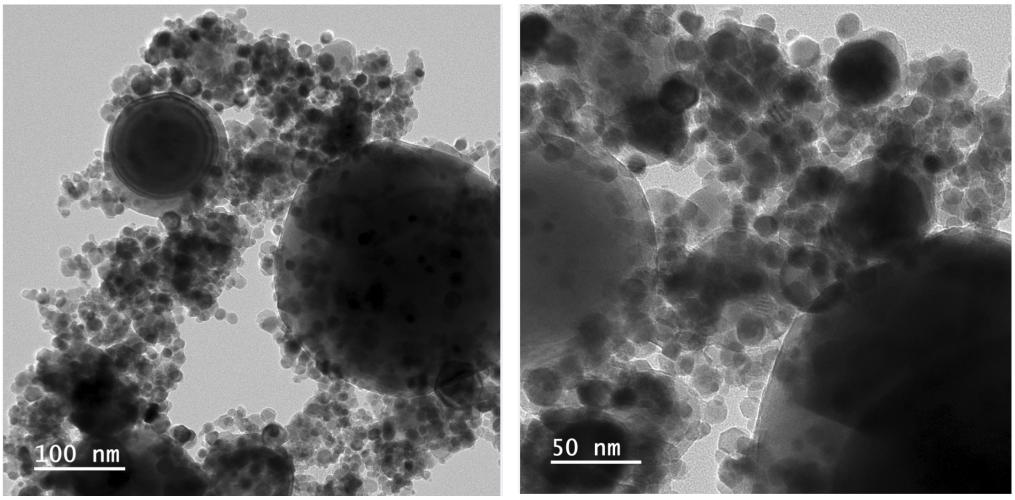

Figure 5. *FETEM images of reduced La(1)-Ni(5)/$AlCeO_3$ catalyst before reaction.*

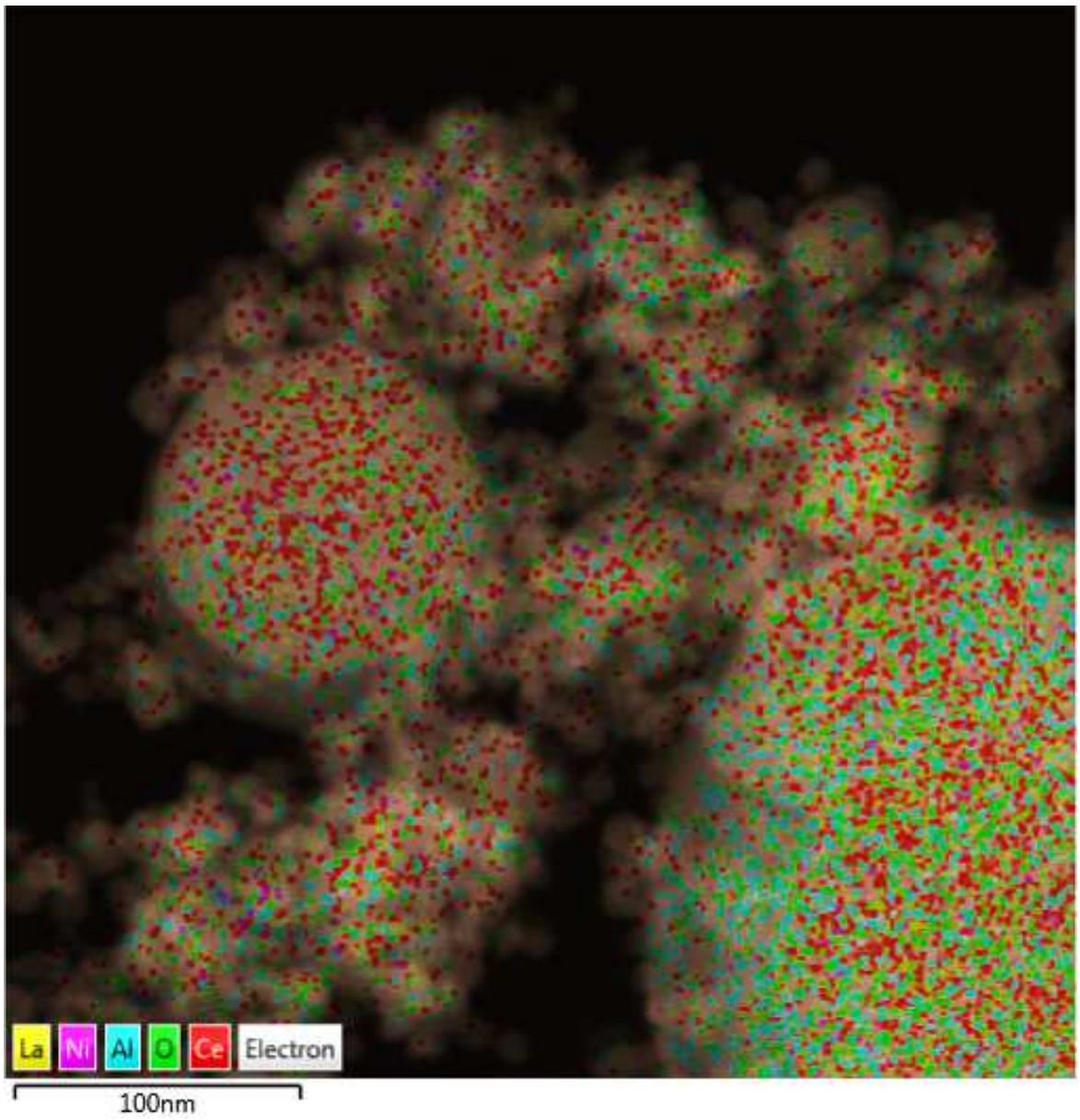

Figure 6. *EDS layered images on surface of reduced La(1)-Ni(5)/$AlCeO_3$ catalyst before reaction.*

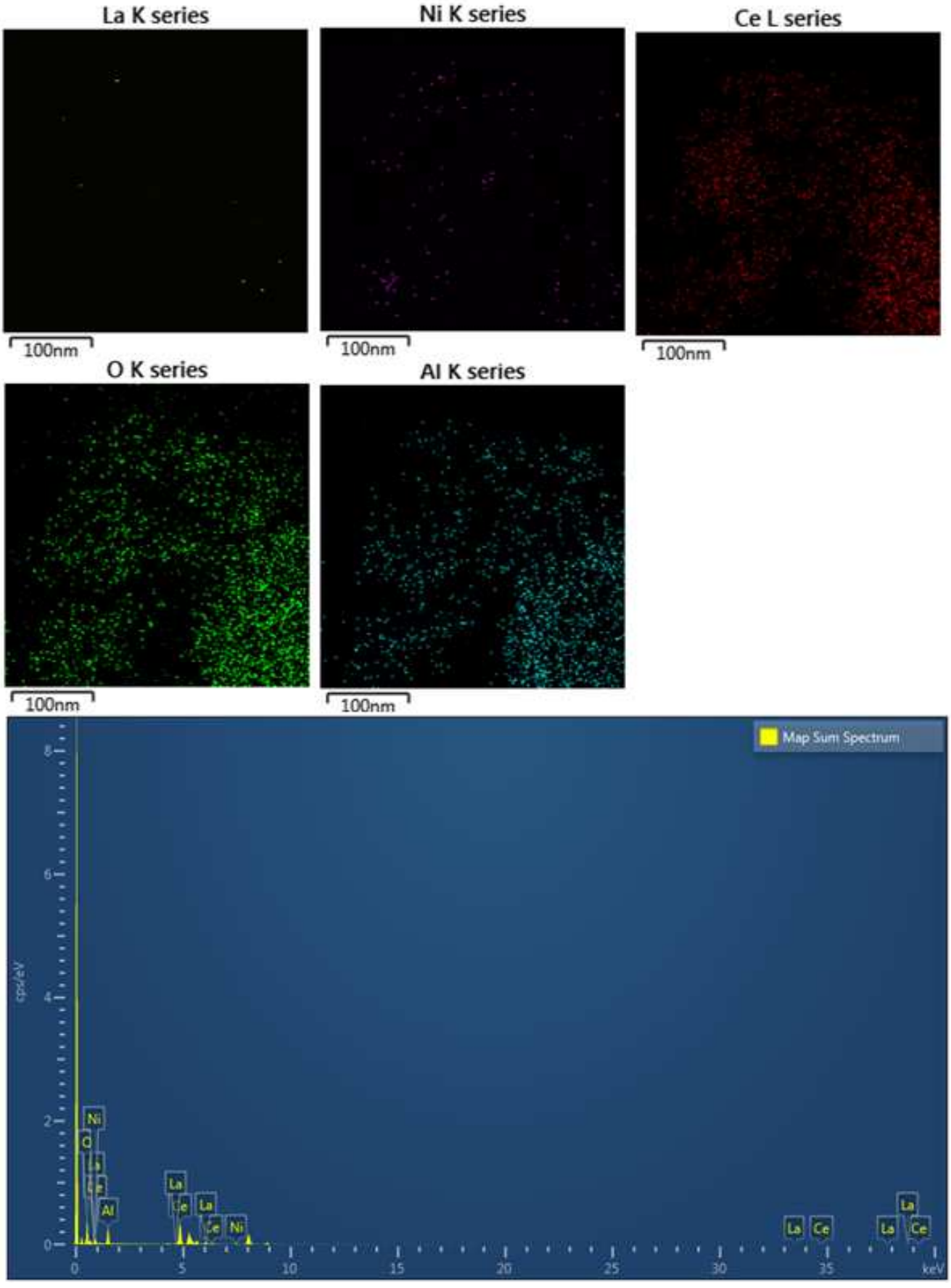

Figure 7. *EDS mapping images on surface of reduced La(1)-Ni(5)/AlCeO$_3$ catalyst before reaction.*

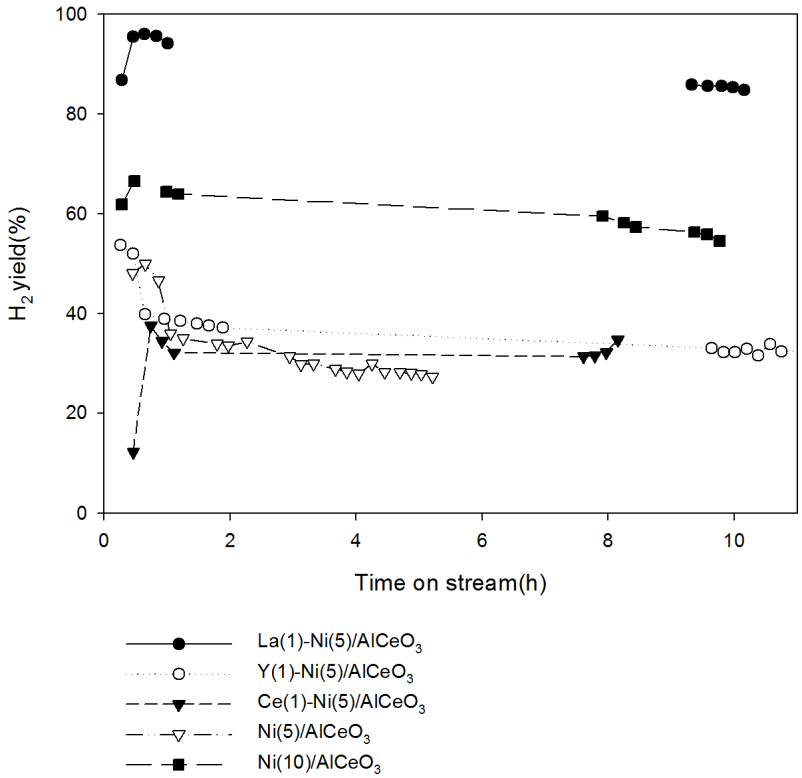

Figure 8. *Yield of H_2 obtained in partial oxidation of methane over M(1)-Ni/Al_2CeO_3(M=La, Y, Ce), Ni(5)/Al_2O_3, and Ni(10)/$AlCeO_3$ catalysts in the packed bed reactor: P=1atm, T=700 ℃, CH_4/O_2=2, and GHSV=1.08 X 10^5 $mLg^{-1}h^{-1}$.*

4. Conclusions

POM was performed over La(1)-Ni(5)/$AlCeO_3$ (M=La, Ce, Y) to investigate the activity of catalysts in hydrogen production and to investigate the active sites of a catalyst. The active sequence of hydrogen yield was La(1)-Ni(5)/$AlCeO_3$>>Ni(10)/$AlCeO_3$>>Y(1)-Ni(5)/$AlCeO_3$> Ce(1)-Ni(5)/$AlCeO_3$> Ni(5)/$AlCeO_3$. It was confirmed that the crystalline phase of Ni and La on reduced La(1)-Ni(5)/$AlCeO_3$ catalyst before reaction was not obserbed due to uniform distribution of nanoparticles by XRD analysis. When 1 wt% of La is added to the Ni(5)/$AlCeO_3$ catalyst, $Ni2p_{3/2}$ and $Ce3d_{5/2}$ increased to 52.7 and 6.3%, respectively. Oxygen vacancies were created due to incorporating La^{3+}, Ni^{2+} into Ce^{4+} ions of CeO_2 made by reacting $AlCeO_3$ and O_2. It increased the dispersion of Ni atoms on the caatalyst and the hydrogen yield through SMSI effect. From the FESEM image, and the EDS characteristic peak of reduced La(1)-Ni(5)/$AlCeO_3$ catalyst before reaction, it can be seen that nanoparticles of Ni, La and Ce are uniformly distributed on the catalyst surface. In addition, TEM images and EDS mapping of La, Ni, Ce, O, and Al for a reduced La(1)-Ni(5)/$AlCeO_3$ catalyst before reaction can be seen that the elements are well distributed.

Conflict of Interest

All the authors do not have any possible conflicts of interest.

References

[1] Dan Welsby, James Price, Steve Pye, Paul Ekins, Unextractable fossil fuels in a 1.5°C world. *Nature.* 2021; 597: 230–234.

[2] Richard A. Kerr, The Many Dangers of Greenhouse Acid. *Science*. 2009; 323: 459.

[3] Anne-Christine Aycaguer, Miriam Lev-On, and Arthur M. Winer, Reducing Carbon Dioxide Emissions with Enhanced Oil Recovery Projects: A Life Cycle Assessment Approach. *Energy Fuels*. 2001; 15 (2): 303-308.

[4] Ray M. Kaplan, Anand N. Vidyashankar, An inconvenient truth: Global worming and anthelmintic resistance. *Veterinary Parasitology*. 2012; 186: 70-78.

[5] Maocai Shen, Wei Huang, Ming Chen, Biao Song, Guangming Zeng, Yaxin Zhang, (Micro)plastic crisis: Un-ignorable contribution to global greenhouse gas emissions and climate change. *Journal of Cleaner Production*. 2020; 254: 120138.

[6] Zheng Li, Guogang Yang, Shian Li, Qiuwan Shen, Facai Yang, Han Wang, Xinxiang Pan, Modeling and analysis of microchannel autothermal methane steam reformer focusing on thermal characteristic and thermo-mechanically induced stress behavior. *International Journal of Hydrogen Energy*. 2021; 46 (38): 19822-19834.

[7] Pan Xu, Zhiming Zhou, Changjun Zhao, and Zhenmin Cheng, Ni/CaO-Al_2O_3 bifunctional catalysts for sorption-enhanced steam methane reforming. *AIChE Journal*. 2014; 60 (10): 2547-3556.

[8] Brigitte R. Devocht, Joris W. Thybaut, NaokiKageyama, Kenneth Toch, Shigeo Tedd Oyama, Guy B. Marin, n Balance between model detail and experimental information in steam methane reforming over a Ni/MgO-SiO_2 catalyst. *AIChE Journal*. 2019; 65 (4): 1222-1233.

[9] Lola Azancot, Luis F. Bobadilla, José L. Santos, José M. Córdoba, Miguel A. Centeno, José A. Odriozola, Influence of the preparation method in the metal-support interaction and reducibility of Ni-Mg-Al based catalysts for methane steam reforming. *International Journal of Hydrogen Energy*. 2019; 44 (36): 19827-19840.

[10] M. Arsalan Ashraf, Oihane Sanz, CristinaItaliano, Antonio Vita, Mario Montes, Stefania Specchia, Analysis of Ru/La-Al_2O_3 catalyst loading on alumina monoliths and controlling regimes in methane steam reforming. *Chemical Engineering Journal*. 2018; 334: 1792-1807.

[11] V. I. Savchenko, A. V. Nikitin, Y. S. Zimin, A. V. Ozerskii, I. V. Sedov, V. S. Arutyunov, Impact of post-flame processes on the hydrogen yield in partial oxidation of methane in the matrix reformer. *Chemical Engineering Research and Design*. 2021; 175: 250-258.

[12] Elif Tezel, Esra Balkanli Unlu, Halit Eren Figen, Sema Z. Baykara, Calcium silicate-based catalytic filters for partial oxidation of methane and biogas mixtures: Preliminary results. *International Journal of Hydrogen Energy*. 2020; 45 (60): 34739-34748.

[13] Cecilia Mateos Pedrero, Silvia González Carrazán, Patricio Ruiz, Preliminary results on the role of the deposition of small amounts of ZrO_2 on Al_2O_3 support on the partial oxidation of methane and ethane over Rh and Ni supported catalysts. *Catalysis Today*. 2021; 363: 111-121.

[14] Farzam Fotovat, Mehrnaz Rahimpour, Comparison and reduction of the chemical kinetic mechanisms proposed for thermal partial oxidation of methane (TPOX) in porous media. *International Journal of Hydrogen Energy*. 2021; 46 (37): 19312-19322.

[15] Zhitao Wang, Yi Cheng, Xin Shao, Jean-Pierre Veder, Xun Hu, Yuyao Ma, Jingjing Wang, Kui Xie, Dehua Dong, San Ping Jiang, Gordon Parkinson, Craig Buckley, Nanocatalysts anchored on nanofiber support for high syngas production *via* methane partial oxidation. *Applied Catalysis A: General*. 2018; 565: 119-126.

[16] Sudhanshu Sharma, Parag A. Deshpande, M. S. Hegde, and Giridhar Madras, Nondeactivating Nanosized Ionic Catalysts for Water-Gas Shift Reaction. *Industrial & Engineering Chemistry Research*. 2009; 48 (14): 6535–6543.

[17] Jianglong Yu, Fu-Jun Tian, and Chun-Zhu Li, Novel Water-Gas-Shift Reaction Catalyst from Iron-Loaded Victorian Brown Coal. *Energy & Fuels*. 2007; 21 (2): 395-398.

[18] Yuanyuan Li, Matthew Kottwitz, Joshua L. Vincent, Michael J. Enright, Zongyuan Liu, Lihua Zhang, Jiahao Huang, Sanjaya D. Senanayake, Wei-Chang D. Yang, Peter A. Crozier3, Ralph G. Nuzzo & Anatoly I. Frenkel, Dynamic structure of active sites in ceriasupported Pt catalysts for the water gas shift reaction. *nature communications*. 2021; 12: 914.

[19] Md Delowar Hossain, Yufeng Huang, Ted H. Yu, William A. Goddard III & Zhengtang Luo, Reaction mechanism and kinetics for CO_2 reduction on nickel single atom catalysts from quantum mechanics. *nature communications*. 2020; 11: 2256.

[20] Rui Huang, Chaesung Lim, Myeong GonJang, Ji Young Hwang, Jeong Woo Han, Exsolved metal-boosted active perovskite oxide catalyst for stable water gas shift reaction. *Journal of Catalysis*. 2021; 400: 148-159.

[21] Chuanmin Ding, Junwen Wang, Songsong Guo, Zili Ma, Yufeng Li, Lichao Ma, Kan Zhang, Abundant hydrogen production over well dispersed nickel nanoparticles confined in mesoporous metal oxides in partial oxidation of methane. *International Journal of Hydrogen Energy*. 2019; 44 (57): 30171-30184.

[22] K. T. de C. Roseno, M. Schmal, R. Brackmann, R. M. B. Alves, R. Giudici, Partial oxidation of methane on neodymium and lanthanium chromate based perovskites for hydrogen production. *International Journal of Hydrogen Energy*. 2019; 44 (16): 8166-8177.

[23] Wei-Hsin Chen, Ting-Wei Chiu, Chen-I. Hung, Hysteresis loops of methane catalytic partial oxidation for hydrogen production under the effects of varied Reynolds number and Damköhler number. *International Journal of Hydrogen Energy*. 2010; 35 (12): 6291-6302.

[24] Xiao Ping Dai, Qiong Wu, Ran Jia Li, Chang Chun Yu, and Zheng Ping Hao, Hydrogen Production from a Combination of the Water-Gas Shift and Redox Cycle Process of Methane Partial Oxidation via Lattice Oxygen over $LaFeO_3$ Perovskite Catalyst. *The Journal of Physical Chemistry B*. 2006; 110 (51): 25856-25862.

[25] Ho Joon Seo, Ung Il Kang, Oh Yun Kwon, Characterization of Pd impregnated on metal/silica-pillared H-keyaites (M-SPK, M=Ti, Zr) catalysts for partial oxidation of methane to hydrogen. *Journal of Industrial and Engineering Chemistry*. 2014; 20 (4): 1332-1337.

[26] Jeongeun Kim, Youngseok Ryou, Tae Hyeop Kim, Gyohyun Hwang, Jungup Bang, Jongwook Jung, Yongju Bang, Do Heui Kim, Highly selective production of syngas (>99%) in the partial oxidation of methane at 480°C over Pd/CeO_2 catalyst promoted by HCl. *Applied Surface Science*. 2021; 560: 150043.

[27] T. J. Siang A. Ajalil, M. Y. S. Hamid, A. A. Abdulrasheed, T. A. T. Abdullah, D. -V. N. Vo, Role of oxygen vacancies in dendritic fibrous M/KCC-1 (M=Ru, Pd, Rh) catalysts for methane partial oxidation to H_2-rich syngas production. *Fuel*. 2020; 278: 118360.

[28] Ramin Jalali, Mehran Rezaei, Behzad Nematollahi, Morteza Baghalha, Preparation of Ni/$MeAl_2O_4$-$MgAl_2O_4$ (Me=Fe, Co, Ni, Cu, Zn, Mg) nanocatalysts for the syngas production via combined dry reforming and partial oxidation of methane. *Renewable Energy*. 2020; 149: 1053-1067.

[29] Halit Eren Figen, Sema Z. Baykara, Effect of ruthenium addition on molybdenum catalysts for syngas production via catalytic partial oxidation of methane in a monolithic reactor. *International Journal of Hydrogen Energy*. 2018; 43 (2): 1129-1138.

[30] Zhitao Wang, Yi Cheng, Xin Shao, Jean-Pierre Veder, Xun Hu, Yuyao Ma, Jingjing Wang, Kui Xie, Dehua Dong, San Ping Jiang, Gordon Parkinson, Craig Buckley, Chun-ZhuLi, Nanocatalysts anchored on nanofiber support for high syngas production *via* methane partial oxidation. *Applied Catalysis A: General*. 2018; 565: 119-126.

[31] Xiaobo Bai, Sheng Wang, Tianjun Sun, Shudong Wang, The sintering of Ni/Al_2O_3 methanation catalyst for substitute natural gas production. *Reaction Kinetcs, Mechanisms and Catalysis*. 2014; 112 (2): 437-451.

[32] Ruiqin Yang, Chuang Xing, Chengxue Lv, Lei Shi, Noritatsu Tsubaki, Promotional effect of La_2O_3 and CeO_2 on Ni/γ-Al_2O_3 catalysts for CO_2 reforming of CH_4. *Applied Catalysis A: General*. 2010; 385 (1-2): 92-100.

[33] Wei-Ping Dow, Yu-Piao Wang, and Ta-Jen Huang, Yttria-stabilized zirconia supported copper oxide catalyst. 1. Effect of oxygen vacancy of support on copper oxide reduction. *Journal of Catalysis*. 1996; 160 (2): 155-170.

[34] Takeshi Miki, Takao Ogawa, Masaaki Haneda, Noriyoshi Kakuta, Akifumi Ueno, Syuji Tateishi, Shinji Matsuura, and Masayasu Sato, Enhanced oxygen storage capacity of cerium oxides in CeO_2/La_2O_3/Al_2O_3 containing precious metals. *The Journal of Physical Chemistry*. 1990; 94 (16): 6464-6467.

[35] Satoshi Sato, Ryoji Takahashi, Mika Kobune, Hiroshi Gotoh, Basic properties of rare earth oxides. *Applied Catalysis A: General*. 2009; 356: 57-63.

[36] H. Ma, L. Zeng, H. Tian, D. Li, X. Wang, X. Li, J. Gong, Efficiency hydrogen production from ethanol steam reforming over La-modified ordered mesoporous Ni-based catalysts. *Applied Catalysis B: Environmental*. 2016; 181: 321-331.

[37] Wallace T. Figueiredo, Guilherme B. Della Mea, Maximiliano Segala, Daniel L. Baptista, Carlos Escudero, Virginia Pérez-Dieste, and Fabiano Bernardi, Understanding the Strong Metal−Support Interaction (SMSI) Effect in CuxNi1−x/CeO_2 (0 < x < 1) Nanoparticles for Enhanced Catalysis. *ACS Applied Nano Materials*. 2019; 2 (4): 2559-2573.

[38] Chun-Jern Pan, Meng-Che Tsai, Wei-Nien Su, John Rick, Nibret Gebeyehu Akalework, Abiye Kebede Agegnehu, Shou-Yi Cheng, Bing-Joe Hwang, Tuning/exploiting Strong Metal-Support Interaction (SMSI) in Heterogeneous Catalysis. *Journal of the Taiwan Institute of Chemical Engineers*. 2017; 74: 154-186.

[39] Bing Han, Yalin Guo, Yike Huang, Dr. Wei Xi, Jie Xu, Prof. Jun Luo, Haifeng Qi, Yujing Ren, Xiaoyan Liu, Prof. Botao Qiao, Prof. Tao Zhang, Strong Metal–Support Interactions between Pt Single Atoms and TiO_2. *Angewandte Chemie Internatonal Editon*. 2020; 59 (29): 11824–11829.

[40] Peiwen Wu, Shuai Tan, Jisue Moon, Zihao Yan, Victor Fung, Na Li, Shi-Ze Yang, Yongqiang Cheng, Carter W. Abney, Zili Wu, Aditya Savara, Ayyoub M. Momen, De-en Jiang, Dong Su, Huaming Li, Wenshuai Zhu, Sheng Dai & Huiyuan Zhu, Harnessing strong metal–Support interactions via a reverse route. *Nature communications.* 2020; 11: 1-10.

[41] Felipe Polo-Garzon, Thomas F. Blum, Zhenghong Bao, Kristen Wang, Victor Fung, Zhennan Huang, Elizabeth E. Bickel, De-en Jiang, Miaofang Chi, and Zili Wu, In Situ Strong Metal–Support Interaction (SMSI) Affects Catalytic Alcohol Conversion. *ACS Catalysis.* 2021; 11 (4): 1938–1945.

[42] Julia Schumann, Maik Eichelbaum, Thomas Lunkenbein, Nygil Thomas, Maria Consuelo Álvarez Galván, Robert Schlögl, and Malte Behrens, Promoting Strong Metal Support Interaction: Doping ZnO for Enhanced Activity of Cu/ZnO: M (M=Al, Ga, Mg) Catalysts. *ACS Catalysis*. 2015; 5 (6): 3260–3270.

[43] C. Alvarez-Galvan, H. Falcs, V. Cascos, L. Troncoso, S. Perez-Ferrera M. Capel-Sanchez, J. M. Campos-Martin, J. A. Alonso, J. L. G. Fierro, Cermets Ni/($Ce_{0.9}Ln_{0.1}O_{1.95}$) (Ln=Gd, La, Nd and Sm) solution combustion method as catalysts for hydrogen production by partial oxidation of methane. *International Journal of Hydrogen Energy.* 2018; 43 (35): 16834-16845.

[44] S. T. Aruna, N. S. Kini, K. S. Rajam, Solution combustion synthesis of CeO_2 -$CeAlO_3$ nano - composites by mixture of fuels approach. *Materials Research Bulletin*. 2009; 44 (4): 728-733.

[45] S. Damyanova, B. Pawelec, R. Palcheva, Y. Karakirova, M. C. C. Sanchez, G. Tyuliev, E. Gaigneaux, J. L. G. Fierro, Structure ans surface properties of ceria-modified Ni-based catalysts for hydrogen production. *Applied Catalysis B: Environmental*. 2017; 225: 340-353.

[46] N. D. Charisiou, G. I. Siakavelas, B. Dou, V. Sebastian, S. J. Hinder, M. A. Baker, K. Polychronopoulou, and M. A. Goula, Nickel Supported on $AlCeO_3$ as a Highly Selective and Stable Catalyst for Hydrogen Production via the Glycerol Steam Reforming Reaction. *Catalysts of MDPI Journals*. 2019; 9: 411-432.

[47] G. Pantalo, V. L. Parola, F. Deganello, R. K. Singha, R. Bal, A. M. Venezia, Ni/CeO_2 cataltsts for methane partial oxidation: Synthesis driven structual and catalytic effects, *Applied Catalysis B: Environmental*. 2016; 189: 233-241.

[48] Ch. Anjaneyulu, S. N. Kumar, V. V. Kumar, G. Naresh, S. K. Bhargava, K. V. R. Chary, and A. Venugopal, Influence of La on reduction behaviour and Ni metal surface area of Ni-Al_2O_3 catalysts for CO_x free H_2 by catalytic decomposition of methane. *International Journal of Hydrogen Energy*. 2015; 40 (9): 3633-3641.